

Sample concentration and impedance detection on a microfluidic polymer chip

Poorya Sabounchi · Alfredo M. Morales · Pierre Ponce · Luke P. Lee · Blake A. Simmons · Rafael V. Davalos

© Springer Science + Business Media, LLC 2008

Abstract We present an on-chip microfluidic sample concentrator and detection triggering system for microparticles based on a combination of insulator-based dielectrophoresis (iDEP) and electrical impedance measurement. This platform operates by first using iDEP to selectively concentrate microparticles of interest based on their electrical and physiological characteristics in a primary fluidic channel; the concentrated microparticles are then directed into a side channel configured for particle detection using electrical impedance measurements with embedded electrodes. This is the first study showing iDEP concentration with subsequent sample diversion down an analysis channel and is the first to demonstrate iDEP in the presence of pressure driven flow. Experimental results demonstrating the capabilities of this platform were obtained using polystyrene microspheres and *Bacillus subtilis* spores. The feasibility of selective iDEP trapping and impedance detection of these particles was demonstrated. The system is intended for use as a front-end unit that can be easily paired with multiple biodetection/

bioidentification systems. This platform is envisioned to act as a decision-making component to determine if confirmatory downstream identification assays are required. Without a front end component that triggers downstream analysis only when necessary, bio-identification systems (based on current analytical technologies such as PCR and immunoassays) may incur prohibitively high costs to operate due to continuous consumption of expensive reagents.

Keywords Dielectrophoresis · Insulator-based dielectrophoresis · Biochip · Sample enrichment · Pathogen monitoring · BioMEMS

1 Introduction

There are many methods to identify biologicals in an aqueous sample, including polymerase chain reaction (PCR), culture or colony counting methods, and immunology-based methods (Lazcka et al. 2007). In order to achieve the required sensitivity, these systems typically utilize a front-end sample concentration step such as mechanical filtration. These methods accurately identify biological particles but may incur high costs in continuous operation due the consumption of expensive reagents. We now demonstrate a system to determine if confirmatory downstream identification assays are required: the system combines a low-cost, relatively high-throughput, and selective front-end concentrator with an early warning non-specific detector to trigger subsequent bioidentification assays.

Dielectrophoresis (DEP) has been used to selectively concentrate microorganisms and serves as an attractive alternative to mechanical filtration because there is no need for back flushing the sample through the filter (Albrecht et al. 2004; Aldaeus et al. 2005; Gadish and Voldman 2006;

P. Sabounchi · P. Ponce · B. A. Simmons (✉)
Energy Systems Department, Sandia National Laboratories,
Livermore, CA, USA
e-mail: basimmo@sandia.gov

P. Sabounchi · L. P. Lee
Berkeley Sensor and Actuator Center,
Department of Bioengineering, University of California,
Berkeley, CA, USA

A. M. Morales
Materials Chemistry Department, Sandia National Laboratories,
Livermore, CA, USA

R. V. Davalos (✉)
School of Biomedical Engineering and Sciences,
Virginia Tech-Wake Forest University,
Blacksburg, VA, USA
e-mail: davalos@vt.edu

Huang and Pethig 1991; Huang et al. 1997; Hughes et al. 1998; James et al. 2006; Pohl 1978). DEP is the motion of a particle in a suspending medium due to the presence of a non-uniform electric field (Pohl 1978). Conventional DEP systems generate electric field gradients by applying an AC signal across two or more metallic electrodes. These systems typically use coplanar electrode (Huang and Pethig 1991; Hughes et al. 1998) or interdigitated (Albrecht et al. 2004; Huang et al. 1997) configurations, and trap particles at or near the electrode surfaces (Aldaeus et al. 2005). Electrode-based DEP systems have been used in various particle analysis systems for sample concentration (Gadish and Voldman 2006; James et al. 2006) and exhibit high selectivity (Aldaeus et al. 2005).

Impedance detection has shown promise as a reliable, inexpensive and reusable method for immediately confirming the presence of particles in solution (Cady et al. 1978; Jonsson et al. 2006; Wawerla et al. 1999; Yang et al. 2004, 2003). The impedance detection exploits changes in the effective complex conductivity of the solution due to differences between the electrical properties of the biological particles and the suspending medium. Since impedance detection uses the unique electrical signatures of particles and the differences in the electrical properties of the particles and the suspending medium, it can provide some information about the nature of the particles. Impedance detection has been used in a number of particle-based microfluidic applications (Gawad et al. 2004; Gomez et al. 2002, Morgan et al. 2006; Sun et al. 2007; Wu et al. 2005).

The concept of conventional dielectrophoresis (DEP) coupled with impedance measurements (DEPIM) has been explored by many researchers (Allsopp et al. 1999, Suehiro et al. 2003a, b, c). Suehiro et al. showed that impedance measurements can be effectively used to detect cells (Suehiro et al. 2003a) when coupled with electroporation of cells (Suehiro et al. 2003c) or with an antibody–antigen reaction (Suehiro et al. 2003b). In these devices, interdigitated metallic electrodes are used to DEP trap particles, which are initially collected on the surface of the electrode (Gomez-Sjoberg et al. 2005; Liu et al. 2007). Formations of linear clusters (a.k.a. “pearls on a string”) of particles develop as particles align themselves through a dipolar effect. Particles are detected by measuring impedance changes due to these “pearl chains” that form an electrical connection between the trapping electrodes. The conductive properties of the particles relative to those of the suspending medium determine the observed changes in impedance, and thus offer a pathway toward identifying the trapped particles.

In insulator-based dielectrophoresis (iDEP), remote electrodes apply an electric field within a volume while insulating obstacles (i.e., packing material [Benguigui and Lin 1984; Lin and Benguigui 1982], or ridges [Barrett et al. 2005; Chou et al. 2002, Davalos et al. Xuan et al. 2005])

distort the electric field producing the spatial non-uniformities needed to enable dielectrophoresis. The potential benefits associated with iDEP include that: there are no embedded metal electrodes, the structure is mechanically robust and chemically inert, electrolysis inside the channel is avoided, and DC fields can be used for DEP and EK flow (Kang et al. 2008). We have previously presented the effectiveness of microfluidic DEP for enrichment and separation of biological particles in a microfluidic channel containing an insulating array of posts (Cummings and Singh 2003; Lapizco-Encinas et al. 2005; Lapizco-Encinas et al. 2004). Devices for iDEP can be made solely from insulating materials (e.g. plastic) which can be replicated inexpensively, facilitating high-throughput large-volume applications (Davalos et al. 2007; Simmons et al. 2006). Although these systems are useful for high-throughput particle removal or concentration, they were not equipped with a detection mechanism that confirmed the presence of particles, thus limiting their utility as an easily integrated component.

In this study we present a robust platform for the concentration and detection of particles in an aqueous solution by combining iDEP with an impedance detection channel. The devices presented in this study are polymer microfluidic chips that are injection molded using a nickel stamp electroplated on a straight-walled, anisotropically etched silicon master. Fabrication of the devices from an anisotropic silicon master enables deep, high-throughput features in the main channel without any degradation in performance of the concentrator since its design features are channel height independent. The electrodes used as impedance sensors in our design are coplanar and rectangular as oftentimes employed in microfluidic applications (Hong et al. 2005; Linderholm and Renaud 2005). The sensing electrodes in our microfluidic chips are passivated with oxide (SiO_2) to avoid the unwanted effects of a direct metal–electrolyte interface at the electrode surface and to maintain system stability for extended periods of time (Sanchis et al. 2007).

This manuscript is the first to demonstrate iDEP concentration with subsequent sample diversion into a detection side channel and is the first to demonstrate iDEP concentration in the presence of pressure driven flow. We demonstrate the efficacy of this system in rapidly concentrating and detecting biological particles through experiments conducted with viable *Bacillus subtilis* spores and polystyrene beads that are similar in size to many prokaryotes. The DEP behavior exhibited by the particles was observed to depend on the magnitude of the applied DC electric field and the physical characteristics of the particles. We demonstrated the feasibility of combining iDEP with impedance detection by conducting a set of experiments using the impedance detection sensor in the secondary side channel. As expected, the impedance detection of these particles was observed to be dependent

on signal frequency and particle concentration. The combination of insulator-based dielectrophoresis (iDEP) with electrical impedance detection as a front-end selective concentrator to trigger a downstream analysis would minimize reagent cost and rapidly alert the end user that something of interest has been collected. Furthermore, our ability to separate viable from non-viable species using iDEP (Lapizco-Encinas et al. 2004) enhances the functionality of the downstream analysis technique—integrating sample identification with viability assessment. The results presented in this study demonstrate the feasibility of iDEP concentration coupled with impedance detection as a low-cost, autonomous, rapid, selective and sensitive concentrator and detector of biological particles.

2 Theory

2.1 Insulator-based dielectrophoresis

DEP is the motion of a particle in a suspending medium due to the presence of a non-uniform electric field (Pohl 1978). The DEP force acting on a spherical particle can be described by the following:

$$\mathbf{F}_{\text{DEP}} = 2\pi\epsilon_m r^3 \text{Re} \left\{ \frac{\tilde{\sigma}_p - \tilde{\sigma}_m}{\tilde{\sigma}_p + 2\tilde{\sigma}_m} \right\} \nabla(\mathbf{E} \cdot \mathbf{E}) \quad (1)$$

where ϵ_m is the permittivity of the suspending medium, r is the radius of the particle, $\nabla(\mathbf{E} \cdot \mathbf{E})$ defines the local electric field gradient, $\tilde{\sigma}_p$ and $\tilde{\sigma}_m$ are the complex conductivities of the particle and the medium, respectively. For frequencies below 100 kHz, the complex conductivities can be approximated in terms of the real conductivities (i.e. $\tilde{\sigma}_i \approx \sigma_i$). When such frequencies are applied and the particles are less conductive than the suspending medium, the particles exhibit “negative” DEP by moving away from regions of high electric field. iDEP systems typically use DC electric fields, and therefore, the dielectrophoretic force exerted on the particles for a given electric field gradient depends on the conductivity of the particle, the conductivity of the medium, and the size of the particle.

The velocity of the particle is the sum of the local liquid velocity and the velocities induced by the particle forces (i.e. dielectrophoresis and electrophoresis). The particle’s dielectrophoretic induced velocity is given by the product of the gradient of the electric field squared, $\nabla(\mathbf{E} \cdot \mathbf{E})$, with the dielectrophoretic mobility, μ_{DEP} :

$$\mu_{\text{DEP}} = \frac{\epsilon_m r^2}{3\eta} \text{Re} \left\{ \frac{\tilde{\sigma}_p - \tilde{\sigma}_m}{\tilde{\sigma}_p + 2\tilde{\sigma}_m} \right\} \quad (2)$$

where η is the viscosity of the medium. The dielectrophoretic mobility is obtained doing a summation of forces and solving for the velocity embedded in the countering

frictional force term due to Stoke’s drag, $f = 6r\pi\eta v$. The trapping threshold is uniquely dependent on the particle type and the solution (i.e. the dielectrophoretic and electrokinetic particle mobility; Davalos et al. 2007; Ermolina and Morgan 2005) and trapping conditions are configurable by adjusting the electric field distribution through modifying the channel geometry and the applied field. For a particle to become trapped in our device, the dielectrophoretic force on the particle must overcome other forces on the particle. Since dielectrophoresis increases as the square of the field and electrokinetic flow only increases linearly with the field, there is an electric field threshold where the dielectrophoretic velocity overcomes the electrokinetic and hydrodynamic velocities of the fluid and the particles will trap.

2.2 Impedance measurements of suspensions

The effective (bulk) conductivity of a dilute suspension of spheres in an electric field can be approximated using the following equation (Maxwell 1873; Wagner 1914):

$$\frac{\tilde{\sigma}_m - \tilde{\sigma}}{2\tilde{\sigma}_m + \tilde{\sigma}} = V(n) \frac{\tilde{\sigma}_m - \tilde{\sigma}_p}{2\tilde{\sigma}_m + \tilde{\sigma}_p} \quad (3)$$

which can be rewritten as

$$\tilde{\sigma}(n) = -\tilde{\sigma}_m \frac{2\tilde{\sigma}_m + \tilde{\sigma}_p - 2V(n)\tilde{\sigma}_m + 2V(n)\tilde{\sigma}_p}{-2\tilde{\sigma}_m - \tilde{\sigma}_p - V(n)\tilde{\sigma}_m + V(n)\tilde{\sigma}_p} \quad (4)$$

where $\tilde{\sigma}(n)$ is the effective complex conductivity of the suspension, and V is volume fraction of particles in the medium, defined as the number of particles times the volume of the particle divided by the volume of the solution.

$$V(n) = \frac{nV_p}{V} \quad (5)$$

where V_p is the volume of a particle, V is volume of the solution and n is the number of particles.

The electrical properties of cells have been studied since the 1940s (Cole 1940; Cole and Cole 1941; Schwan 1957). From an electrical perspective, a cell is essentially a conductive medium with a highly conductive cytoplasm encapsulated by an ultrathin low conductivity barrier, the cell membrane (Davalos et al. 2000, 2002). Assuming that the thickness of the membrane is negligible relative to the radius of the cell, (3) can be extended to cells by using the following equation for the complex conductivity of the cell:

$$\tilde{\sigma}_p = \frac{\tilde{\sigma}_i - (2d/r)(\tilde{\sigma}_i - \tilde{\sigma}_o)}{(1 + d/r)(\tilde{\sigma}_i - \tilde{\sigma}_o)/\tilde{\sigma}_o} \quad (6)$$

where d is the thickness of the membrane, $\tilde{\sigma}_i$ is the complex conductivity of the cell interior, and $\tilde{\sigma}_o$ is the complex conductivity of the cell membrane (Fricke 1955; Grimnes and Martinsen 2000).

Equation (3) is exact in the first order of V and only valid for dilute suspensions. However, it was experimentally (Foster and Schwan 1986) and numerically (Pavlin and Miklavcic 2003; Pavlin et al. 2002) shown that this approximation also holds well for higher volume fractions; i.e., high density particle suspensions.

3 Experimental section

Channel and Electrode Design The particle trapping efficiency of an iDEP device is directly related to: (1) the particle size, (2) the relative difference in complex conductivity between the particle and the suspending medium, and (3) the nonuniform electric field. The electric field is applied by remote electrodes and the nonuniformity of the electric field is induced by insulating structures in the microchannel. Furthermore, the relative difference in electrical properties between the particles and the solution can be exploited to detect the presence of particles using impedance detection. Our microfluidic system (Fig. 1) operates by selectively concentrating pathogens of interest based on their size in the main fluidic channel using insulator-based dielectrophoresis. Each device contains a main channel for high-throughput processing of the sample and selective particle concentration, bisected by a perpendicular analysis channel for sensitive detection of the released concentrated sample (Fig. 1). The main microchannel is 1 mm wide, 20 mm long and 90 μm deep and contains one set of insulating structures to induce dielectrophoresis for particle trapping. The first and last columns of the post are tapered to reduce fouling. The post is arranged in either a 4×4 or 5×5 arrays. The main channel is

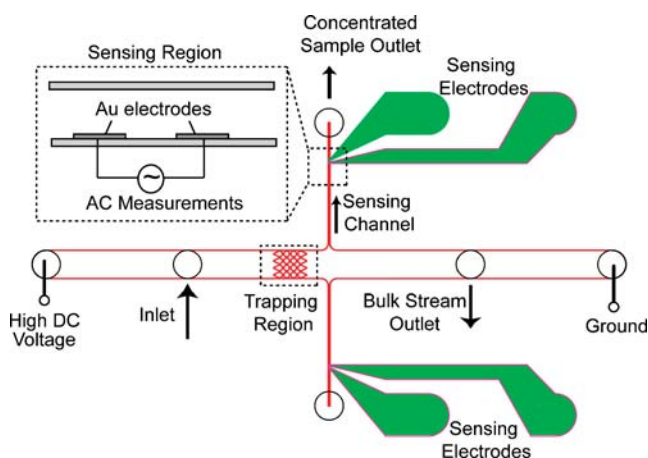


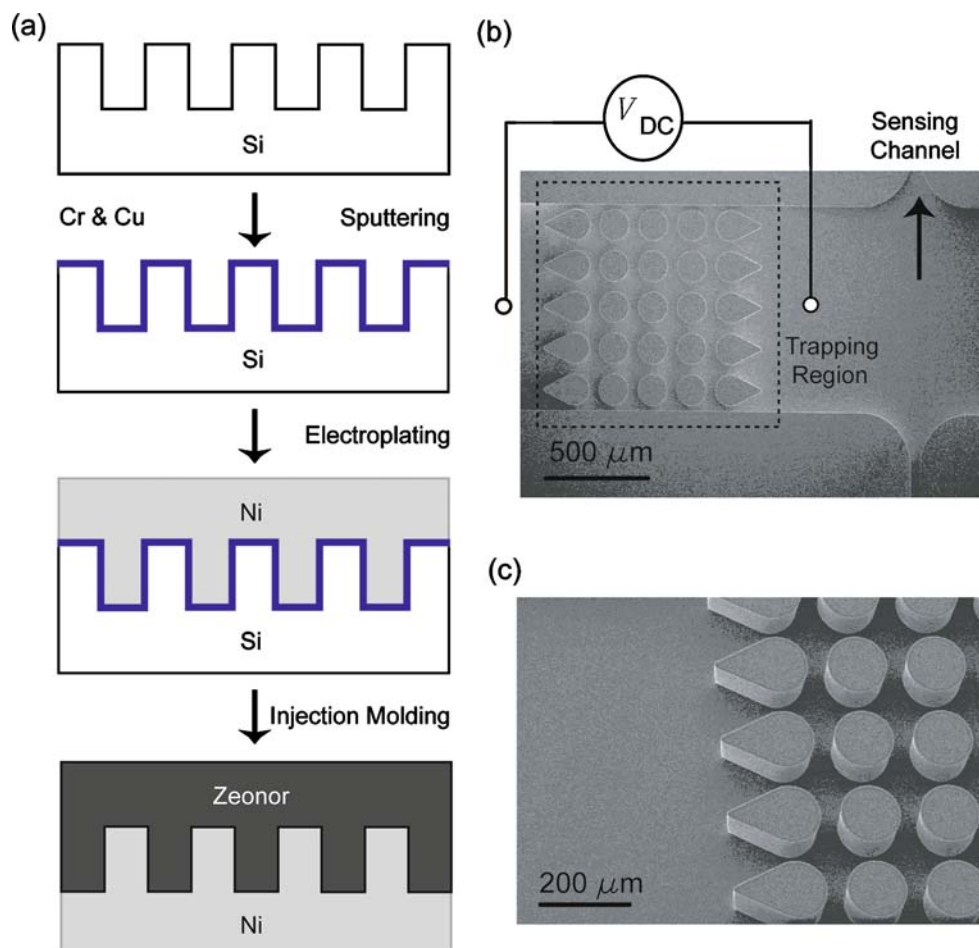
Fig. 1 Schematic of iDEP coupled with impedance measurements: The microfluidic device operates by selectively concentrating pathogens of interest based on their size using insulator based dielectrophoresis (iDEP) in the main fluidic channel using high DC voltage followed by releasing the concentrated sample to a side channel for AC impedance measurement using pressure-driven flow

equipped with four ports: one to supply the voltage, an inlet port, an outlet port, and ground. Four outlets are used to avoid any direct contact of the metal electrodes with the sample. The analysis channel is 50 μm wide, 10 mm long and 90 μm deep. The analysis channel contains two sets of electrodes on either side of the main channel. The detection sites within the channel consists of two 50 μm coplanar rectangular electrodes, separated by 150 μm (center-to-center), as depicted in Fig. 1(a). Typical device operation is as follows: (1) A particle-containing solution is introduced into the main fluidic channel, (2) an electric field (DC) of sufficient magnitude is applied across the main channel, (3) after the targeted particles have been concentrated for a predetermined amount of time the electric field is reduced, releasing the trapped particles, and the concentrated particles are delivered to a side channel to detect the presence or absence of a pathogen using impedance measurement. Because the particle suspension has a higher conductivity relative to the solution, the conductivity in the microfluidic sensing region will increase when particles are present. This measurement can be used to estimate the number of particles collected by dielectrophoresis.

Microfluidic polymer substrate fabrication The microfluidic channel for our testing platform is fabricated in Zeonor™ 1060, a cyclic olefin copolymer available from Zeon Chemicals (Louisville, KY; Fig. 2). The fabrication process starts by patterning a 100 mm diameter silicon wafer master with straight sidewall channels and posts using reactive Bosch etching. After patterning, the master is sputter-coated with an electroplating base consisting of 500 Å thick chromium (adhesion layer) and 1,500 Å thick copper (actual plating surface). The master is then placed in a Digital Matrix commercial DM3M electroplating machine running a commercial nickel sulfamate bath (Technic, San Jose, CA). Electroplating is carried out at 48°C for a total of 40 A h and produces one millimeter thick nickel films. The electroplated nickel is then machined to the dimensions required to fit in our injection molding equipment, a 60-ton TH-60 vertical injection molding machine (Nissei® America, Los Angeles, CA). Zeonor™ 1060R resin pellets are dried at 40°C for at least 24 h prior to use. The pellets are then fed to the injection molding barrel through a gravity-assisted external hopper. The cycle time for molding one 100 mm diameter Zeonor™ wafer is approximately 2 min. Visual inspection using cross-polarized optical filters is used to assess and minimize residual stresses in the injection molded parts. Figure 2(b) and (c) show scanning electron microscope (SEM) images of the Zeonor™ microfluidic substrates.

Polymer lid fabrication, impedance electrode deposition, and bonding One hundred millimeters round discs turned from commercially available, injection molded 1.6-mm thick Zeonor® 1060R plaques (Zeon Chemicals, Louisville,

Fig. 2 Microfluidic device fabrication: (a) Fabrication steps of injection molded polymer microfluidic device. Deep reactive ion etching (DRIE) was used to prepare the Si which was then used as a substrate for electroplating of a Ni stamp. (b) SEM image of unbonded polymer microfluidic device showing the insulating posts and the sensing channel (c) Close up SEM image of unbonded polymer posts in the main channel



KY) are used as lids to seal the injection molded microfluidic substrates. One millimeter diameter vias are drilled through the discs using a Uniline-2000 drill (Excellon Automation Co., Rancho Dominguez, CA) to provide a fluidic interface to the ports depicted in Fig. 1.

The impedance electrodes are deposited using two metal shadow masks. The first shadow mask, which has four 1 mm×1 mm contact pads per device was placed over the substrates containing the microfluidic channels. Metal (~0.4 μm thick Au) was then thermally evaporated onto the substrate in the pattern formed by the shadow mask. The second shadow mask, which has the pattern for the impedance electrodes in contact with the solution, was placed directly onto the lid. The metal material for the electrodes was thermally evaporated (~0.4 μm thick Au film) in the pattern contained in the shadow mask. The surfaces of the lids were then sputtered with a ~0.4 μm thick oxide layer (SiO₂), covering the impedance electrode surface, to prevent the occurrence of electrolysis in the solution and protect the sensing electronics. By avoiding a direct metal-electrolyte interface with the oxide passivation layer, we ensure that the

system behavior remains stable for extended periods of time and little or no calibration is needed (Sanchis et al. 2007).

The microfluidic channel substrate is then thermally bonded to the lids using a Carver press (Carver, Inc., Wabash, IN). Bonding is typically carried out as follows: the lid and the substrate are visually aligned and manually brought into contact; they are placed in the press at ambient temperature; the press is then heated to 190°F while applying a load of 750 psi g; the sample is held at this pressure and temperature for 60 min; the bonded assembly is then cooled to 75°F under constant load and removed from the press. All bonded assemblies were checked for flow and channel blockage before use.

Microfluidic interface The completely assembled system was controlled by laptop. A standardized breadboard (Labsmith, Livermore, CA) was used for mounting and positioning components (Fig. 3(a)). Flow was driven by a custom made syringe pump powered by a stepper motor which was controlled by LabVIEW (National Instruments, Austin, TX). The experiments were monitored using an

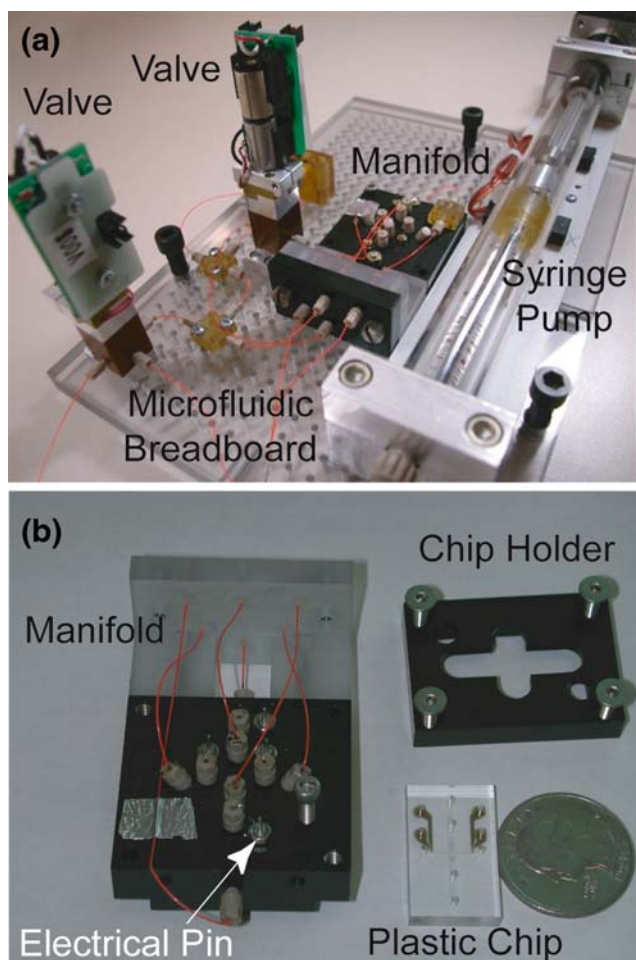


Fig. 3 Microfluidic interface: (a) A breadboard is used for mounting and positioning fluidic components. Particles are driven by a custom made syringe pump and routed into the sensing channel using custom made valves which are all controlled by a microprocessor-controlled main system board. (b) A Delrin polymeric microfluidic manifold with integrated O-ring seals provides the interface between the microfluidic chip and fluid reservoirs. High voltage electronics and impedance measurement interconnects are supplied to microfluidic reservoirs through platinum electrodes connected to a multi-pin electrode connector

inverted epifluorescence Olympus IX-70 microscope (Olympus, Center Valley, PA) employing an Olympus 4102 fluorescence filter set. A Delrin polymeric, compression microfluidic manifold with integrated O-ring seals provided the interface between the chips and fluid reservoirs (Fig. 3(b)). Delrin was chosen because it is easily machined and is chemically resistant. Holes (0.25 mm diameter) were drilled through the manifold to match the microfluidic chip fluid access hole pattern. One manifold face contained 0.61 mm inner diameter and cross section dovetail-captured Buna-N O-rings (Apple Rubber Products., Lancaster, NY) Fused-silica capillaries (30 mm long, 150 μm i.d., 365 μm o.d.; Polymicro Technologies, Phoenix, AZ) provided fluidic connections between the chip and the reservoir cartridge and attached to the compression manifold on the

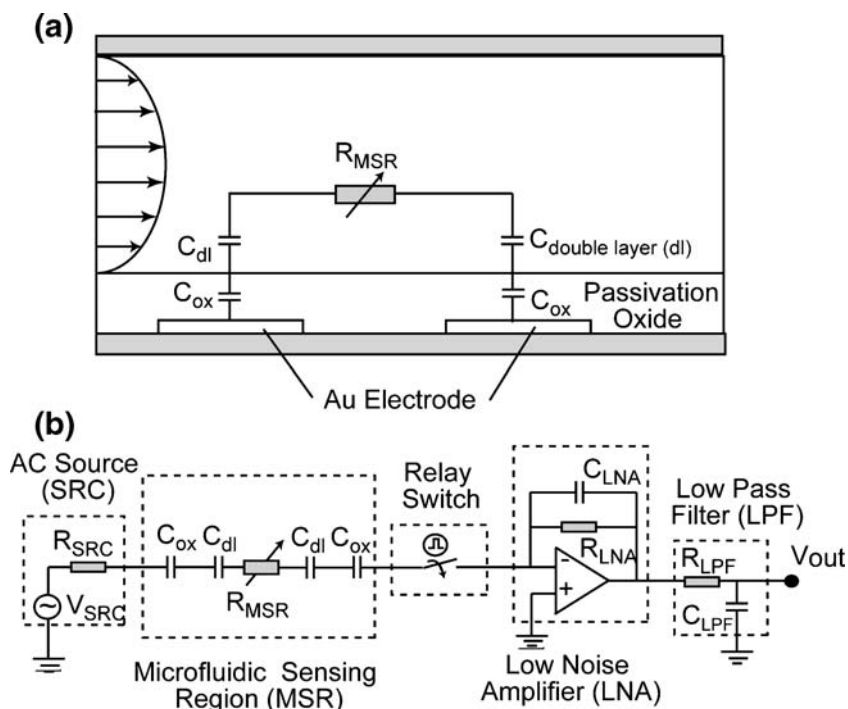
face opposite to the O-rings (the top face) using custom-designed one-piece polyetheretherketone (PEEK) fittings (Fig. 3(b)). The capillaries were recessed into the manifold top face to prevent capillary damage. Four electronically actuated multi-port high pressure valves with swept volumes of less than 10 nL were used for routing.

The sample was introduced into the chip through a pressure injection port on the side of the compression manifold. The injection port and chip sample loop were connected by a 200 nL O-ring sealed viaduct machined into the compression manifold. High voltage was supplied to reservoir fluids through platinum electrodes (Omega Engineering Inc, Stamford, CT) connected to a multi-pin electrode connector. Electrodes were made from stainless steel disks laser-welded to 2 cm-long platinum wires, which were inserted through the reservoir cartridge top and extend into each reservoir fluid chamber. The electrode connector attached to the reservoir cartridge top and consisted of a polyphenylene sulfide plate with spring-loaded pins (Everett Charles Technologies, Pomona, CA) that made contact with the reservoir electrodes (Fig. 3(b)). The microchannel was primed by flowing buffer solution at a rate of 100 $\mu\text{L}/\text{min}$. This flow rate was maintained until all air bubbles within the channel were removed. Flow was then reduced to the normal experimental rate (30 $\mu\text{L}/\text{min}$) following the priming process.

Particles and Solutions Suspensions of *B. subtilis* spores were obtained from Raven Biological Laboratories Inc. (Omaha, NE). The spore solutions were then diluted between 1:20 and 1:100 by volume in pH- and conductivity-controlled deionized water. Carboxylate-modified polystyrene microspheres (Molecular Probes, Eugene, OR) having a density of 1.05 mg/mm^3 and diameters of 2 μm were utilized at a dilution of 3:10,000 from a 2% by wt. stock suspension. Bead suspensions were sonicated between steps of serial dilution and before use. The background solution was deionized water obtained from a reverse osmosis filter titrated with KOH and HCl to a pH of approximately 8. Conductivity was then adjusted by titration with KCl to an endpoint of 1–2 $\mu\text{S}/\text{cm}$.

Electronics for iDEP and impedance measurements A programmable high voltage power supply, HVS448 (Lab-Smith, Livermore CA), was employed to provide high voltage during the measurement, and current variation was recorded every 20 ms using a laptop and Sequence software program (LabSmith). The HVS448 provided feedback to the main system board for active current control. Full-scale stepped voltages can be generated in 20 ms, and precise applied voltages and measured currents are updated and displayed every 50 ms providing either fixed voltage or current capability. The microprocessor-controlled main system board included a menu-based user interface, modular

Fig. 4 Impedance measurements detect the presence or absence of a pathogen: (a) Simplified electrical model of the impedance change in the sensing channel when particles are present. (b) Schematic of the test circuit used to measure impedance changes in the microfluidic device. A relay switch was used during the application of the iDEP voltage to decouple the effect of high voltage on the impedance measurement. A radio frequency lock-in amplifier (not shown) was used to demodulate and amplify signal at each frequency

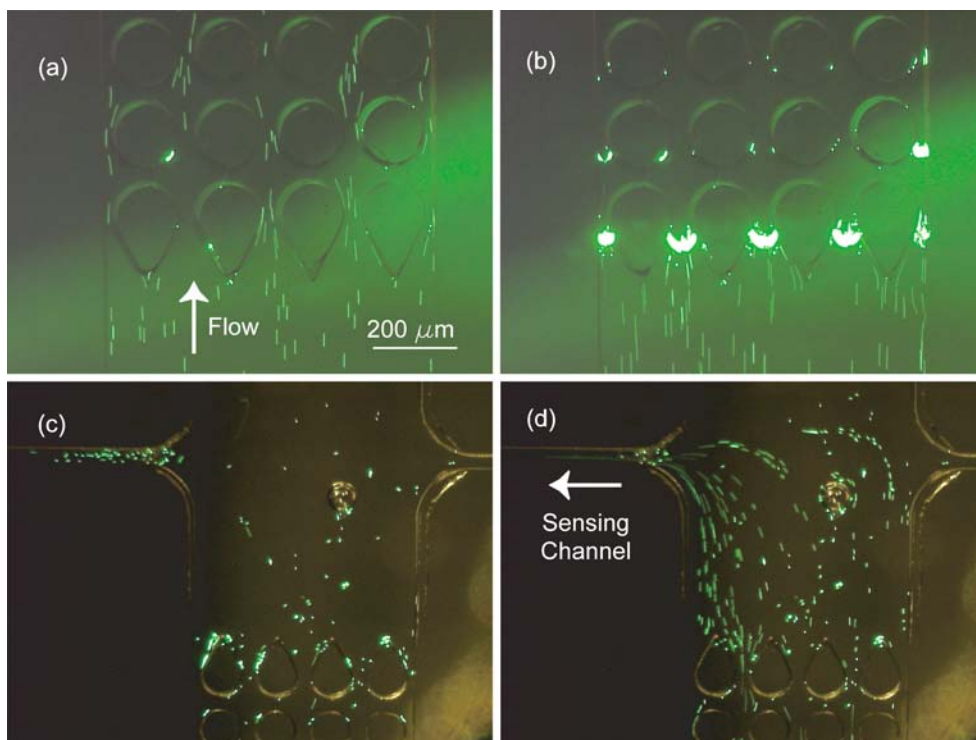


power supply connections, system control software, impedance data acquisition and processing functions, and instrument communications. The main board also included two 12-bit A/D converters for reading power supply currents, impedance signal, and power supply voltages, which were all provided through an analog multiplex device. D/A con-

verters are used to set power supply bias voltages. An 8-bit Rabbit 2000 microprocessor (Rabbit Semiconductor, Davis, CA) performs all control operations including low-level and real-time microfluidic interfacing and data acquisition.

The flow of individual particles within the medium can be modeled as variable impedance, as shown in Fig. 4(a).

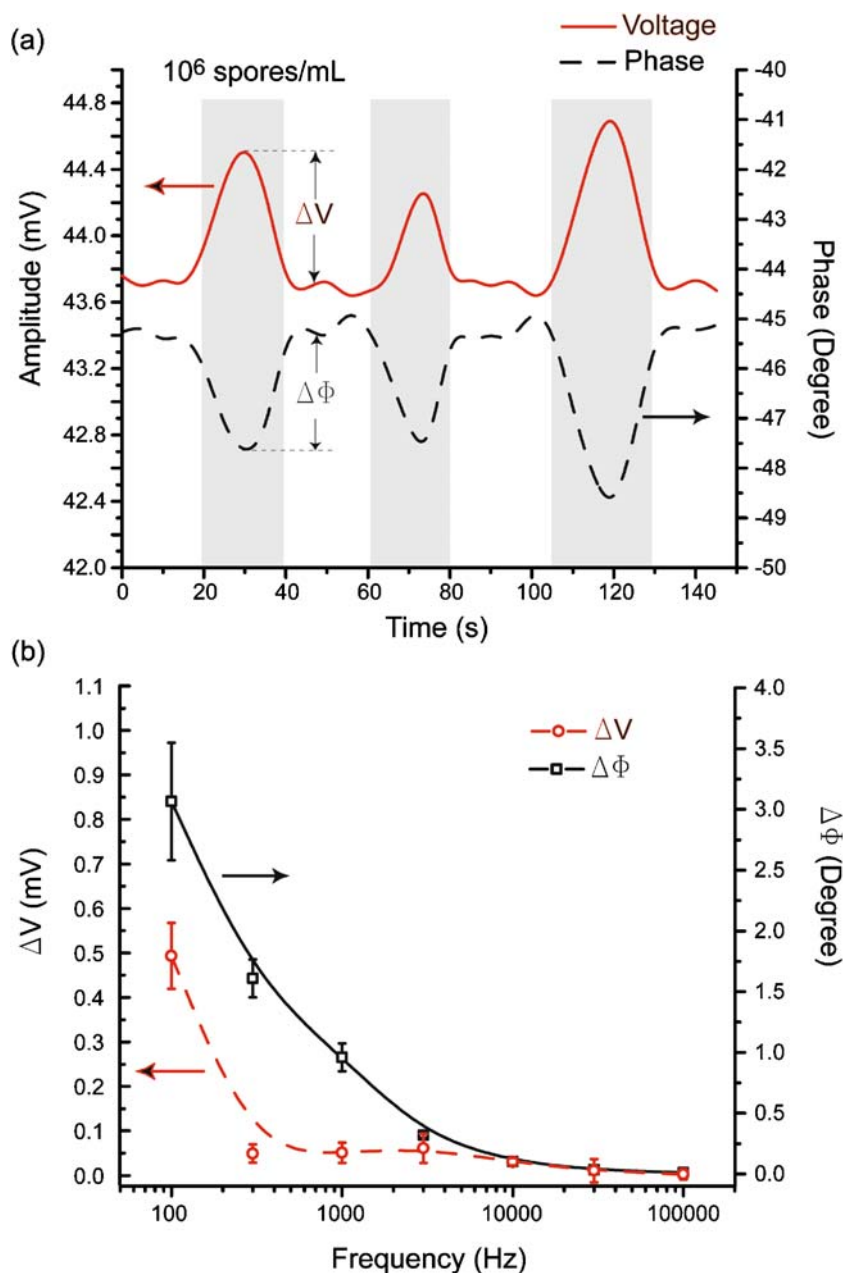
Fig. 5 Insulator-based dielectrophoretic concentration and shuttling of sample: (a) Individual particle (2- μm fluorescent beads) types were injected into the microchannel at an injection rate of 10 $\mu\text{L}/\text{min}$, while the normal experimental buffer flow rate of 30 $\mu\text{L}/\text{min}$ was maintained. The applied voltage across the microchannel was increased to 1,000 V until incipient iDEP trapping was observed at the trapping region, mostly at the post array inlet (b) with very few beads flowing out of the post array outlet (c). (d) Following iDEP trapping, the voltage was dropped and the particles were diverted to the side channel for impedance measurement



The schematic of the test circuit used to measure impedance changes in the microfluidic device is detailed in Fig. 4(b). An AC probe signal of 100 mV amplitude (RMS) was used as a source. A relay switch was used during the application of the DEP voltage to decouple the effect of high voltage on the impedance measurement. A low noise amplifier (Stanford Research Systems, Sunnyvale, CA) that performs as a low-pass filter at a frequency one decade higher than the input signal was used to enhance the signal-to-noise ratio. A radiofrequency lock-in amplifier (SR830 DSP Stanford Research Systems, Sunnyvale, CA) was used to demodulate and amplify signal at each frequency. The lock-in amplifier outputs are capacitively connected to a digital

acquisition board (DAQ6024E, National Instruments, Austin, TX, USA) providing sampling of eight inputs at up to 105 samples/s. The direct-current levels for each of the demodulated signals are acquired separately through digital GPIB connections to the lock-in amplifier. As before, electrical contact to the electrodes on-chip was made through holes drilled through the lid using spring-loaded pins. Sample injection and separation times, applied voltages or currents, and impedance measurement are user-defined for each analysis channel. Individual analysis channels are independently controlled. Individual node voltages can be adjusted during instrument operation by changing their values via the user menu. The resulting data

Fig. 6 Real-time impedance detection of *B. subtilis* spores: **(a)** *B. subtilis* spores at a concentration of 10^6 particles/mL where diverted into the sensing channel three times for period of 10 s and the output signal (V_{out}) were measured. The grey area demonstrates the time that most concentrated portion of sample plug is detected. The applied voltage was a 100 mV amplitude (RMS) sine wave oscillating at 100 Hz. **(b)** Effect of frequency on impedance characteristics using a 100mV amplitude (RMS) sine wave



are typically displayed in real time and stored for post processing on a laptop computer running LabVIEW (National Instruments, Austin, TX).

4 Results and discussion

In order to evaluate the performance of the autonomous platform, we use fluorescent polystyrene beads, which are analogous to biological particles, to determine the capability of the system to selectively remove particles of interest from the sample stream. While maintaining the normal experimental buffer flow rate of 30 $\mu\text{L}/\text{min}$, fluorescent beads with a diameter of 2 μm were injected into the microchannel at an injection rate of 10 $\mu\text{L}/\text{min}$ (Fig. 5(a)) for a total flow rate of 40 $\mu\text{L}/\text{min}$. After increasing the voltage across the microchannel to 1000V, dielectrophoretic concentration of the beads was observed at the trapping region (Fig. 5(b), (c)). After approximately 1 min, the voltage was dropped and the trapped beads were routed to the side channel for impedance measurement (Fig. 5(d)) by switching the microprocessor-controlled three-way valves.

After the sample is diverted down the side channel, impedance detection is enabled by monitoring impedance changes through sensing electrodes within the channel. To test our system, we diverted *B. subtilis* spore suspensions at a concentration of 10^6 per mL through the detection channel for periods of 10 s and then washed the side channel with a constant buffer flow. Values of the amplitude and phase of the output (V_{out}) were recorded at a sampling period of 125 ms (Fig. 6). Three measurements were taken at each of the frequencies tested for a total of 21 experiments. The applied voltage was a 100 mV amplitude (RMS) sine wave oscillating at 100 Hz. Since we are using a low conductivity buffer (DI water, 1–2 $\mu\text{S}/\text{cm}$), when a suspension of the biological particles passes through the microfluidic sensing region there is a drop in the resistance between the electrodes. Lowering the resistance between the electrodes results in more current through the system as depicted in Fig. 4. This current flows through the internal resistance of the lock-in amplifier and creates an increased output voltage (Fig. 6(a)). Figure 6(a) shows that measuring phase is more suitable for detecting biological particles than amplitude because there is a greater relative change, which is typical in bioimpedance (Grimnes and Martinsen 2000). We verified these trends by measuring the impedance of the *B. subtilis* spore in sample vials off-line.

We then varied the applied frequency of the measuring signal to determine which frequency resulted in a more pronounced change in signal. Figure 6(b) shows impedance (amplitude and phase) offsets at varying frequencies using a 100 mV (RMS) input sinusoidal signal. As expected, at lower frequencies the offsets were more pronounced, and

therefore more sensitive to changes in particle concentration. At high frequencies, the presence of stray capacitances in parallel with the measurement sample will shunt the channel impedance and affect the device sensitivity by decreasing signal-to-noise ratio. The results in Fig. 6 indicate that the system is suitable for detecting suspensions of 10^6 spores per milliliter.

In order to characterize the effect of concentration on impedance measurement *B. subtilis* spores at concentration levels ranging from 10^1 to 10^5 spores per milliliter were diverted to the side channel and changes in phase were measured (Fig. 7). Three measurements were taken at each concentration tested for a total of 12 experiments. As expected, the change in phase is more pronounced with higher particle concentration. As the concentration of particles increases, the displacement of solution by those particles leads to larger changes in the impedance of the sensing region. These findings imply that if the application for this technology is to selectively concentrate and divert only one particle type, the impedance measurements can approximate the concentration of the particles diverted down the channel. In this system, a syringe pump can initially inject a calibration sample (with a known concentration and particle conductivity) into the chip and record the impedance results while a pump can provide continuous buffer solution. This would allow the real crude sample to be injected afterwards to measure its concentration with an established baseline value to mitigate the number of false positives and negatives.

The results in Fig. 7 show that the impedance detection system can detect samples concentrated to dilutions as low

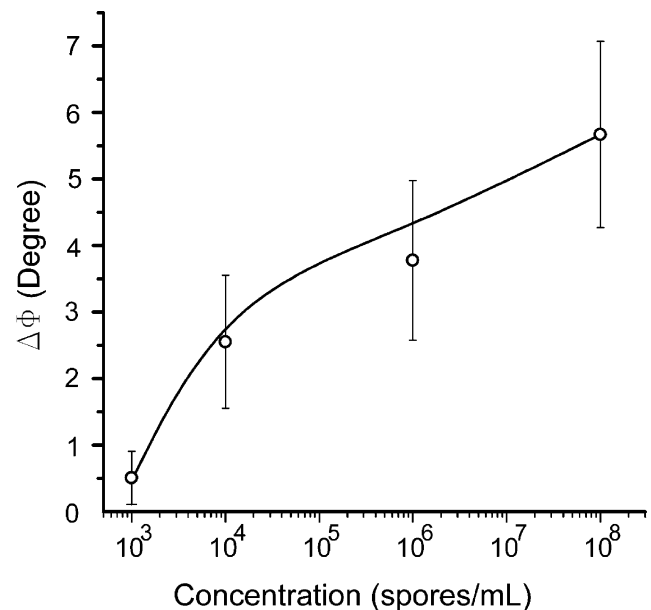


Fig. 7 The effect of particle concentration on impedance detection: The analytes were viable *B. subtilis* spores. The applied voltage was a 100 mV amplitude (RMS) sine wave oscillating at 100 Hz. As expected, the change in phase increases with particle concentration

as 10^3 – 10^4 particles per mL. We have demonstrated the effectiveness of iDEP at achieving two to three orders of concentration depending on the length of the concentration step (Davalos et al. 2004, 2007; Lapizco-Encinas et al. 2005). The results in Fig. 7 suggest that the lower limit of our methodology of combining iDEP with impedance detection would be on the order of detecting initial dilutions injected at 40 μ L per minute of ten spores per milliliter. However, it should be emphasized that these studies are preliminary and further studies need to be conducted to define performance limits and compare this methodology to existing technologies.

5 Conclusion

We designed the microfluidic platform to selectively enrich particles using iDEP so that the concentrated sample would be within the detection limits of an integrated bioimpedance technique. We demonstrated the feasibility of coupling iDEP with impedance detection through reliable enrichment and diversion of particles and the impedance mapping between phase offset and particle concentration. We envision a role of this polymeric microdevice as a cost-effective and disposable tool used in multiple front-end sample preparation applications that will enhance current detection techniques.

Another advantage of this technology is that the concentrator is used as a high-throughput filter in addition to being a concentrator for the detector. Since the particles are concentrated in one area and then detected in another area, only the concentrated particles of interest are detected while contaminants and debris are removed or reduced. This filter can be turned on or off quickly and at will without clogging or performance degradation. Furthermore, since the concentrator uses insulating structures as a selective non-clogging filter for picking out specific particles, there is no direct electrode contact with the fluid in the trapping area where particles are concentrated.

Acknowledgments The authors thank J. Van de Vreugde, A. Salmi, K. L. Krafcik, J.L. Caldwell, J. Hachman, B. Crocker, J. Brazzle, S. Ferko, Y. Syed, and J. Rognlien for their contributions to this project. Sandia is a multiprogram laboratory operated by Sandia Corporation, a Lockheed Martin Company, for the US Department of Energy's National Nuclear Safety Administration under contract DEAC04-94AL85000.

References

- D.R. Albrecht, R.L. Sah, S.N. Bhatia, *Biophys. J.* **87**, 2131 (2004)
 F. Aldaeus et al., *Electrophoresis* **26**, 4252 (2005)
 D.W.E. Allsopp et al., *J. Phys. D Appl. Phys.* **32**, 1066 (1999)
 L.M. Barrett et al., *Anal. Chem.* **77**, 6798 (2005)
 L. Benguigui, I.J. Lin, *J. Appl. Phys.* **56**, 3294 (1984)
 P. Cady et al., *J. Clin. Microbiol.* **7**, 265 (1978)
 C.-F. Chou et al., *Biophys. J.* **83**, 2170 (2002)
 K.S. Cole, Cold Spring Harbor Symp. Quant. Biol. **8**, 110 (1940)
 K.S. Cole, R.H. Cole, *J. Chem. Phys.* **9**, 341 (1941)
 E.B. Cummings, A.K. Singh, *Anal. Chem.* **75**, 4724 (2003)
 R. Davalos, Y. Huang, B. Rubinsky, *Microscale Thermophys. Eng.* **4**, 147 (2000)
 R.V. Davalos, et al., in *MicroTAS 2004, A performance comparison of post- and ridge-based dielectrophoretic particle sorters* (Malmo, Sweden, 2004), p. 650
 R.V. Davalos et al., *Anal. Bioanal. Chem.* **389**, 1426 (2007)
 R.V. Davalos, B. Rubinsky, D.M. Otten, *IEEE Trans. Biomed. Eng.* **49**, 400 (2002)
 I. Ermolina, H. Morgan, *J. Colloid Interface Sci.* **285**, 419 (2005)
 K.R. Foster, H.P. Schwan, Dielectric properties of tissues, in *Handbook of Biological Effects of Electromagnetics Fields*, ed. by C.P.A.E. Postow (CRC, Florida, 1986)
 H. Fricke, *J. Phys. Chem.* **59**, 168 (1955)
 N. Gadish, J. Voldman, *Anal. Chem.* **78**, 7870 (2006)
 S. Gawad et al., *Lab Chip* **4**, 241 (2004)
 R. Gomez-Sjoberg, D.T. Morissette, R. Bashir, *J. Microelectromech. Syst.* **14**, 829 (2005)
 R. Gomez, R. Bashir, A.K. Bhunia, *Sens Actuators B* **86**, 198 (2002)
 S. Grimnes, Ø.G. Martinsen, *Bioimpedance and Bioelectricity Basics* (Academic, New York, 2000)
 J. Hong et al., *Lab Chip* **5**, 270 (2005)
 Y. Huang, R. Pethig, *Meas. Sci. Technol.* **2**, 1142 (1991)
 Y. Huang et al., *Biophys. J.* **73**, 1118 (1997)
 M.P. Hughes et al., *Biochim. Biophys. Acta* **1425**, 119 (1998)
 C.D. James et al., *J. Fluids Eng.* **128**, 14 (2006)
 M. Jonsson et al., *J. Phys. Chem. B* **110**, 10165 (2006)
 Y. Kang, et al., *Biomed. Microdevices* **10**, 243–249 (2008)
 B.H. Lapizco-Encinas et al., *J. Microbiol. Methods* **62**, 317 (2005)
 B.H. Lapizco-Encinas et al., *Anal. Chem.* **76**, 1571 (2004)
 O. Lazcka, F.J.D. Campo, F.X. Munoz, *Biosens. Bioelectron.* **22**, 1205 (2007)
 I.J. Lin, L. Benguigui, *J. Electrostat.* **13**, 257 (1982)
 P. Linderholm, P. Renaud, *Lab Chip* **5**, 1416 (2005)
 Y.-S. Liu et al., *Lab Chip* **7**, 603 (2007)
 J. Maxwell, *Treatise on electricity and magnetism* (Oxford University Press, London, 1873)
 H. Morgan, D. Holmes, N.G. Green, *Curr. Appl. Phys.* **6**, 367 (2006)
 M. Pavlin, D. Miklavcic, *Biophys. J.* **85**, 719 (2003)
 M. Pavlin, T. Slivnik, D. Miklavcic, *IEEE Trans. Biomed. Eng.* **49**, 77 (2002)
 H. Pohl, *Dielectrophoresis* (Cambridge University Press, Cambridge, 1978)
 A. Sanchis et al., *Bioelectromagnetics* **28**, 393 (2007)
 H.P. Schwan, *Adv. Biol. Med. Phys.* **5**, 147 (1957)
 B.A. Simmons et al., *Mater. Res. Bull.* **31**, 120 (2006)
 J. Suehiro et al., *J. Electrostat.* **57**, 157 (2003a)
 J. Suehiro et al., *J. Electrostat.* **58**, 229 (2003b)
 J. Suehiro et al., *Sens. Actuators B* **96**, 144 (2003c)
 T. Sun et al., *Lab Chip* **7**, 1034 (2007)
 K.W. Wagner, Explanation of the dielectric fatigue phenomenon on the basis of Maxwell's concept, in *Arkiv für Electrotechnik*, ed. by H. Shering (Springer, Berlin, 1914)
 M. Wawerla et al., *J. Food Prot.* **62**, 1488 (1999)
 J. Wu, Y. Ben, H.-C. Chang, *Microfluid. Nanofluid.* **1**, 161 (2005)
 X. Xuan, B. Xu, D. Li, *Anal. Chem.* **77**, 4323 (2005)
 L. Yang et al., *Biosens. Bioelectron.* **19**, 1139 (2004)
 L. Yang, C. Ruan, Y. Li, *Biosens. Bioelectron.* **19**, 495 (2003)